International Journal of Science Academic Research
Vol. 03, Issue 05, pp.3877-3884, May, 2022
Available online at http://www.scienceijsar.com

ISSN: 2582-6425

Research Article

MODELING FOR PIEZOELECTRIC ACTUATOR WITH DISSIMILAR MATERIALS

***Dong-Chan Lee**

IAE, 175-28, Goan-ro 51 beon-gil, Baegam-myeon, Cheoin-gu, Yongin-si, Gyeonggi-do, 17180, Korea

Received 24th March 2022; **Accepted** 29th April 2022; **Published online** 30th May 2022

Abstract

This paper presents the numerical modeling of a piezoelectric actuator. The vibro-elastic piezoelectric actuator has the layered structures. Applying the equivalent parameters based on the plate/shell theories to the multilayered structures, it is possible to investigate the geometric and material characteristics of multilayered systems and estimate their structural performances. And the optimization designs for the geometric dimensions or material properties of multilayered systems on the layered model can easily be achieved.

Keywords: Multilayered systems, Flexural stiffness, Structural damping, Bimorph model.

INTRODUCTION

The multilayered systems are commonly used in macro-scale or micro-scale applications such as active structural damping or excitation and precision positioning systems. The formulations of actuator configurations which are composed of the piezoelectric layers and non-piezoelectric layers are very important for the conceptual design. The geometric configuration of the layered system is very important for the structural design with low cost, high performance and quality. Particularly, some layered systems will be designed to minimize weight and to achieve a high stiffness such as sandwich beams or plates. For the layered systems subjected to bending, the effective mechanical properties such as flexural stiffness can be determined using the rule of mixtures and are dependent on the layer configurations. These devices are sufficient for determining the quasi-static behavior of the system since the layers are relatively thin. For the development of multilayered systems, the main assumptions of plate/shell theories, which allow for transverse shear deformation effects, are that the displacements are small compared to the plate thickness, the stress normal to the plate mid-surface is negligible, and normal to the mid-surface remain straight but not necessarily normal to the mid-surface after deformation. Ross-Ungar-Kerwin equations (Ross *et al.,* 1959), single element modeling based on variation asymptotical or symmetric theory (Agnes, 1995; Wang and Cross, 1999) and transfer matrix procedure (Nashif *et al.,* 1985; DeVoe and Pisano, 1997; Hwang and Park, 1993; Oka *et al.,* 1991) have been developed to describe the layered material treatment. This paper presents this effective approach to estimate the layer configurations and flexural stiffness of multilayered materials. The concept can be developed to describe the flexural stiffness of more complex multilayer configurations containing these materials, with different layer thickness and spaces and with symmetric or asymmetric layer distributions. It may be possible to estimate the physical and mechanical properties and multi-material multilayered structures.

Theoretical considerations for the multilayered systems

The theory of plates and shells (Ugural and Fenster, 1995) assumes that sections normal to the middle plane remain plane during the deformation and the normal stresses in z direction are small as shown in figure 1, hence strains in that direction can be neglected.

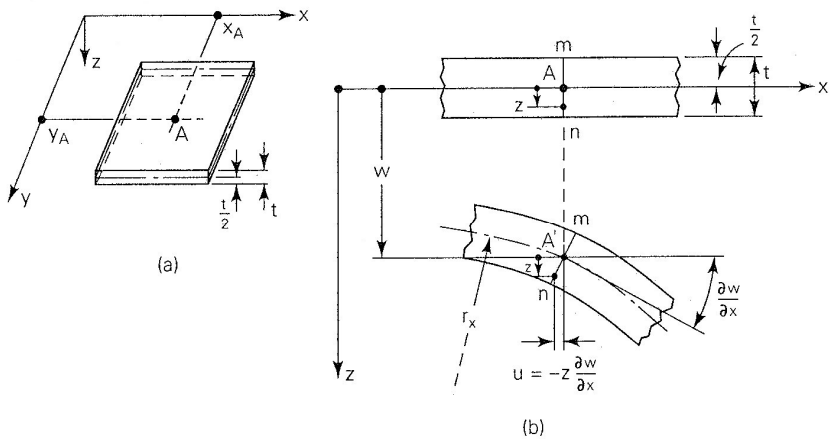

Figure 1. Deformation of a plate in bending

Corresponding Author:** ***Dong-Chan Lee
IAE, 175-28, Goan-ro 51 beon-gil, Baegam-myeon, Cheoin-gu, Yongin-si, Gyeonggi-do, 17180, Korea.

With these two assumptions it is easy to see that the total state of deformation can be described as follows. From the assumption that the normal strain ε_z owing to vertical loading may be neglected, the local displacements in the direction of x, y and z axes are,

$$\begin{aligned} u &= -z\frac{\partial w}{\partial x} + f_2(x,y) \text{ with } \gamma_{xz} = \partial w/\partial x + \partial u/\partial z = 0 \\ v &= -z\frac{\partial w}{\partial y} + f_3(x,y) \text{ with } \gamma_{yz} = \partial w/\partial y + \partial v/\partial z = 0 \\ w &= f_1(x,y) \qquad \text{with } \varepsilon_z = \partial w/\partial z = 0 \end{aligned} \tag{1}$$

It is clear that f_2 and f_3 represent, respectively, the values of u and v corresponding to $z = 0$. Because of an in-plane strain, $f_2 = f_3 = 0$. The stress components σ_x, σ_y and $\tau_{xy} = \tau_{yx}$ are related to the strains by Hooke's law, which for a thin plate becomes,

$$\begin{aligned} \sigma_x &= -\frac{Ez}{1-\nu^2}\left(\frac{\partial^2 w}{\partial x^2} + \nu\frac{\partial^2 w}{\partial y^2}\right) \\ \sigma_y &= -\frac{Ez}{1-\nu^2}\left(\frac{\partial^2 w}{\partial y^2} + \nu\frac{\partial^2 w}{\partial x^2}\right) \\ \tau_{xy} &= -\frac{Ez}{1+\nu}\frac{\partial^2 w}{\partial x \partial y} \end{aligned} \tag{2}$$

The stresses distributed over the side surfaces of the plate, while producing no net force, do result in bending and twisting moments. These moment resultants per unit length are denoted by M_x, M_y and M_{xy}. The bending and twisting moments per unit length are,

$$\begin{aligned} M_x &= \int_{-t/2}^{t/2} z\,\sigma_x\, dz \\ M_y &= \int_{-t/2}^{t/2} z\,\sigma_y\, dz \\ M_{xy} &= \int_{-t/2}^{t/2} z\,\tau_{xy}\, dz \end{aligned} \tag{3}$$

Introducing into Eq. (3) the stresses given by Eq. (2), and taking into account the fact that $w = w(x,y)$, we obtain

$$\begin{aligned} M_x &= -D\left(\frac{\partial^2 w}{\partial x^2} + \nu\frac{\partial^2 w}{\partial y^2}\right) \\ M_y &= -D\left(\frac{\partial^2 w}{\partial y^2} + \nu\frac{\partial^2 w}{\partial x^2}\right) \\ M_{xy} &= -D(1-\nu)\frac{\partial^2 w}{\partial x \partial y} \end{aligned} \tag{4}$$

where $D = \dfrac{Et^3}{12(1-\nu^2)}$ is the flexural stiffness of the single plate. The relationship of the bending curvature with the bending moment can be given by,

$$\frac{1}{r_x} E\, I = M_b \tag{5}$$

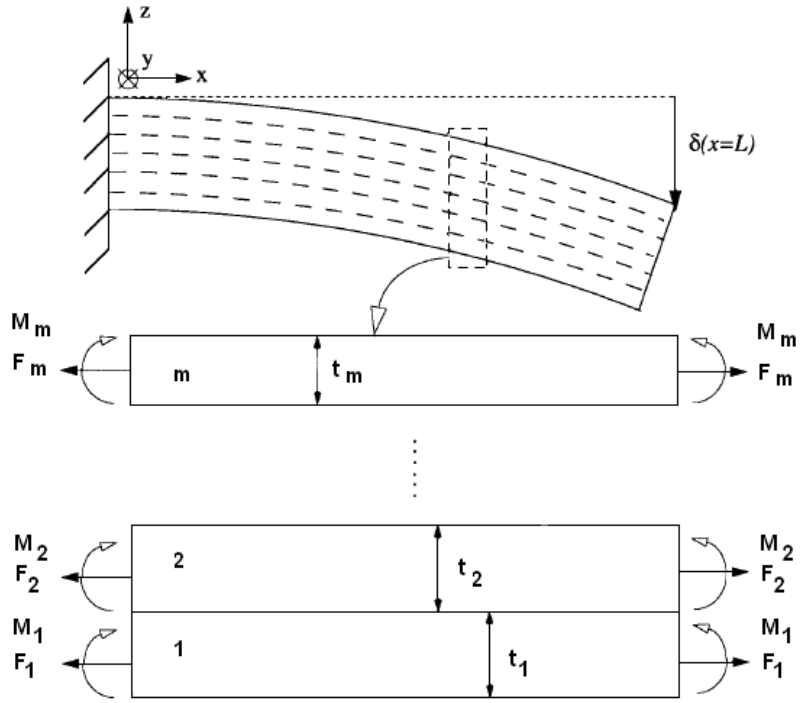

Figure 2. General multilayered configurations

The multilayered configurations are shown in figure 2 and since the layer thickness is much less than the overall plate curvature, the radius of curvature is approximately equal for each layer in the structure.. With the above assumptions of single plate, it is noted that both axial forces and moments at any cross section of the m-layer plate shown in figure 2 must sum to zero at equilibrium (Ugural and Fenster, 1995; Lee, 2004).

$$\sum_{i=1}^{m} Fi = 0,\ \sum_{i=1}^{m} Mi = F_1\left(\frac{t_1}{2}\right) + F_2\left(t_1 + \frac{t_2}{2}\right) + \cdots + F_m\left(\sum_{i=1}^{m-1} t_i + \frac{t_m}{2}\right) = M_b \quad (6)$$

Under the identical bending moment, the radius of curvature is the same for the deformation behavior. [9]

$$\frac{1}{r_x}\sum_{i=1}^{n} E_i I_i = M_b = F_1\left(\frac{t_1}{2}\right) + F_2\left(t_1 + \frac{t_2}{2}\right) + \cdots + F_m\left(\sum_{i=1}^{m-1} t_i + \frac{t_m}{2}\right)$$

$$\frac{1}{r_x} = \frac{1}{\sum_{i=1}^{n} E_i I_i} M_b = \frac{1}{\sum_{i=1}^{n} E_i I_i}\left[F_1\left(\frac{t_1}{2}\right) + F_2\left(t_1 + \frac{t_2}{2}\right) + \cdots + F_m\left(\sum_{i=1}^{m-1} t_i + \frac{t_m}{2}\right)\right] \quad (7)$$

$$\equiv \{D\}^T \{F\}$$

where $\{D\}^T = \frac{1}{\sum_{i=1}^{n} E_i I_i}\left\{\left(\frac{t_1}{2}\right)\left(t_1 + \frac{t_2}{2}\right)\cdots\left(\sum_{i=1}^{m-1} t_i + \frac{t_m}{2}\right)\right\}$, $\{F\} = \begin{Bmatrix} F_1 \\ F_2 \\ \vdots \\ F_m \end{Bmatrix}$

Since the dissipation can be integrated over all layers, the equivalent critical damping ratio is yielding the following expression.

$$\varsigma_{eq} = \frac{1}{E_{eq} t_{eq}^{\ 3}} \sum_{i=1}^{n} \varsigma_i E_i t_i^{\ 3} \quad (8)$$

where $E_{eq} t_{eq}^{\ 3} = \sum_{i=1}^{n} E_i t_i^{\ 3}$ and the critical damping ratio of layers, ς_i, can be derived from the modal test or numerical solutions.

The structural damping is calculated as $C_s = 2\varsigma$.

The total strain at the surface of each layer can be given by superposition due to the piezoelectric effect, axial force and bending moment (Ugural and Fenster, 1995; Uchino, 1997). This surface strain can be given by eq. (9). The sign of the train due to bending will depend on whether the top or bottom face of the layer is under observation.

$$\varepsilon_i = \varepsilon_{\text{piezo}} + \varepsilon_{\text{axial}} + \varepsilon_{\text{bend}} = d_{31}E^p{}_i + \frac{F_i}{A_iE_i} \pm \frac{t_i}{2r} \tag{9}$$

$\varepsilon_{\text{piezo}}$ in the linear constitutive equation above considers the transverse piezoelectric coupling coefficient d_{31} and the electric field across the thickness of the layer $E^p{}_i$ for a piezoelectric material. The strain at the interface layer between the i-th and (i+1) shown in figure 2, the can be given by,

$$d_{31}E^p{}_i + \frac{F_i}{A_iE_i} - \frac{t_i}{2r} = d_{31}E^p{}_{i+1} + \frac{F_{i+1}}{A_{i+1}E_{i+1}} + \frac{t_{i+1}}{2r} \tag{10}$$

$$\frac{F_i}{A_iE_i} - \frac{F_{i+1}}{A_{i+1}E_{i+1}} - \frac{1}{2r}\left(t_i + t_{i+1}\right) - d_{31}\left(E^p{}_{i+1} - E^p{}_i\right) = 0 \tag{11}$$

Collecting similar terms and placing the result into matrix form yields the expression.

$$\left[AE\right]\{F\} - \frac{1}{2r}\{T\} - d_{31}\left\{E^p\right\} = \{0\} \tag{12}$$

where $\left[AE\right]$ is the matrix consisting of A_iE_i and the Young's modulus E_i can have the probabilistic distributions (Lee *et al.,* 2005) due to the manufacturing environments($E_i = \left(1 - \alpha\overline{\rho}\right)E^o{}_i$ for the linear distribution, $E_i = E^o{}_i e^{-\alpha\overline{\rho}}$ for the exponential distribution, $E_i = E^o{}_i\left(1 - \frac{\alpha\overline{\rho}}{1 + (\alpha - 1)\overline{\rho}}\right)$ for semi-empirical distribution), $\{T\}$ is the vector of $t_i + t_{i+1}$ and $\left\{E^p\right\}$ is the vector of $E^p{}_{i+1} - E^p{}_i$.

Using eq. (7) and (12), the curvature yields,

$$\frac{1}{r} = \frac{2d_{31}\{D\}^T\left[AE\right]^{-1}\left\{E^p\right\}}{2 - \{D\}^T\left[AE\right]^{-1}\{T\}} \tag{13}$$

From eq. (13), the deflection of a simple cantilever beam with constant curvature is calculated.

$$\delta(x) = \frac{x^2}{2r} = x^2\left(\frac{d_{31}\{D\}^T\left[AE\right]^{-1}\left\{E^p\right\}}{2 - \{D\}^T\left[AE\right]^{-1}\{T\}}\right) \tag{14}$$

Applications to piezoelectric actuator

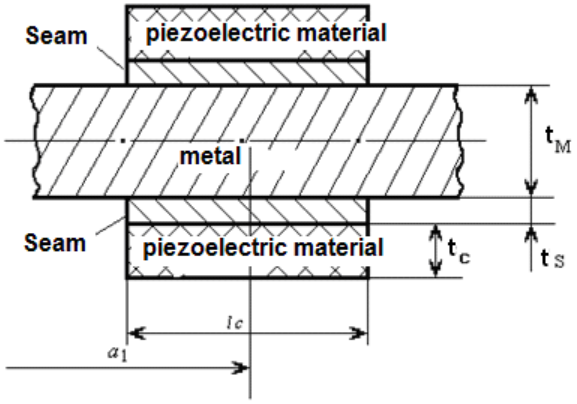

Figure 3. Schematic configuration of dither spoke.

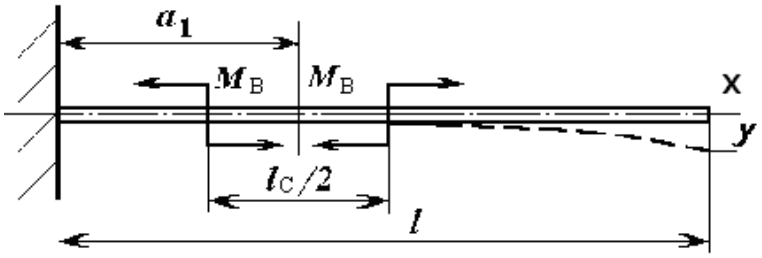

Figure 4. Bending configuration of dither spoke

The tension and compression forces are created by the piezoelectric layers symmetrically bonded to the top and bottom surfaces of non-piezoelectric layer shown in figure 3, and depend on its geometric dimensions, piezoelectric properties and the electrical voltage V supplied to the piezoelectric elements (Vetrov *et al.,* 1999),

$$F_{\mathrm{c}} = \frac{\varepsilon\varepsilon_0 S_c E^p}{d_{31}} = \frac{\varepsilon\varepsilon_0 S_{\mathrm{c}}}{d_{31}} \frac{V}{t_{\mathrm{c}}} \tag{15}$$

where ε is the relative dielectric permeability of the piezoelectric, ε_0 is the dielectric constant, S_c is the transverse section area of the piezoelectric elements, E^p is the piezoelectric field $\left(V/t_c\right)$, t_c is the thickness of the piezoelectric element, , and d_{31} is the piezoelectric constant.

Under the micro operation condition of elastic metal actuator [13, 14], the piezoelectric attached to the elastic metal prevents the bending motion of elastic metal actuator due to the increased equivalent rigidity. Therefore, the optimal thickness dimension ratio between piezoelectric and elastic metal actuator has to be studied. Pressure-sensitive element is a cantilever type, which has the rotational angle and linear transverse deflection. The bending rigidity of bimorph element shown in figure 4 can be written as

$$\left(EI_x\right)_1 = \left(E_{\mathrm{M}} + E_{\mathrm{S}} \frac{I_{\mathrm{S}}}{I_{\mathrm{M}}} + E_{\mathrm{C}} \frac{I_{\mathrm{C}}}{I_{\mathrm{M}}}\right) \cdot I_M = E_e I_M \ , \left(a_1 - \frac{l_{\mathrm{C}}}{4}\right) < x < \left(a_1 + \frac{l_{\mathrm{C}}}{4}\right) \tag{16}$$

$$\left(EI_x\right)_2 = E_{\mathrm{M}} I_M \ , \left(a_1 + \frac{l_{\mathrm{C}}}{2}\right) < x < l$$

The equivalent elastic modulus of bimorph element is given by.

$$E_{\mathrm{e}} = E_{\mathrm{M}} + E_{\mathrm{S}} \frac{I_S}{I_{\mathrm{M}}} + E_{\mathrm{C}} \frac{I_{\mathrm{C}}}{I_{\mathrm{M}}}, \tag{17}$$

where E_{C} is the elastic modulus of piezoelectric, E_M is the elastic modulus of metal, E_S is the elastic modulus connective seam,

$I_S = 2\left[\frac{w_C t_S^3}{12} + w_C t_S \left(\frac{t_M}{2} + \frac{t_S}{2}\right)^2\right]$ is the transverse inertial moment of section area of connective seams for the neutral axis,

$I_C = 2\left[\frac{w_C t_C^3}{12} + w_C t_C \left(\frac{t_M}{2} + t_S + \frac{t_C}{2}\right)^2\right]$ is the transverse inertial moment of section area of piezoelectric element for the neutral axis,

$I_M = \frac{w_M t_M^3}{12}$ is the transverse inertial moment of section area of metal for the neutral.

Without the consideration of inertial force, the transverse deflection according to the length of elastic actuator can be written by.

$$\delta(x)=\frac{M_{\mathrm{b}}}{(EI_x)_1}\cdot\frac{\left(x-a_1+\frac{l_{\mathrm{C}}}{4}\right)^2}{2},\ \left(a_1-\frac{l_{\mathrm{C}}}{4}\right)<x<\left(a_1+\frac{l_{\mathrm{C}}}{4}\right) \tag{18}$$

$$\delta(x)=\frac{M_{\mathrm{b}}}{(EI_x)_1}\frac{\left(x-a_1+\frac{l_{\mathrm{C}}}{4}\right)^2}{2}-\frac{M_{\mathrm{b}}}{(EI_x)_1}\frac{\left(x-a_1-\frac{l_{\mathrm{C}}}{4}\right)^2}{2},\ \left(a_1+\frac{l_{\mathrm{C}}}{4}\right)<x<\left(a_1+\frac{l_{\mathrm{C}}}{2}\right) \tag{19}$$

$$\delta(x)=\delta_{\mathrm{a_1+\frac{l_C}{2}}}\frac{x}{a_1+\frac{l_{\mathrm{C}}}{2}},\ \left(a_1+\frac{l_{\mathrm{C}}}{2}\right)<x<l, \tag{20}$$

Without the consideration of the rigidity increase due to the piezoelectric layers and connective seams, the total transverse deflection is given from.

$$\delta(l)=A_1\frac{t_{\mathrm{M}}+t_{\mathrm{C}}+2t_{\mathrm{S}}}{2t_{\mathrm{C}}}\cdot\frac{l_{\mathrm{C}}}{l}\left(1-\frac{a_1}{l}\right)l=A_1\left(\frac{t_{\mathrm{M}}}{2t_{\mathrm{C}}}+\frac{1}{2}+\frac{t_{\mathrm{S}}}{t_{\mathrm{C}}}\right)\cdot\frac{l_{\mathrm{C}}}{l}\left(1-\frac{l_{\mathrm{C}}}{2l}\right)l \tag{21}$$

where $A_1=\dfrac{\varepsilon\varepsilon_0 S_{\mathrm{c}}V}{(EI_x)_2 d_{31}}$, $a_1=\dfrac{l_C}{2}$ (22)

Assuming $\chi=\dfrac{t_{\mathrm{C}}}{t_{\mathrm{M}}}$ and $\lambda=\dfrac{l_{\mathrm{C}}}{l}$, eq. (21) is rewritten as.

$$\delta(l)=A_2\left[\frac{1}{2\left(t_{\mathrm{C}}/t_{\mathrm{M}}\right)}+\frac{1}{2}+\frac{t_{\mathrm{S}}}{t_{\mathrm{M}}\cdot\left(t_{\mathrm{C}}/t_{\mathrm{M}}\right)}\right]$$

$$=\frac{A_2}{2}\left[\frac{1}{\chi}\left(1+2\frac{t_{\mathrm{S}}}{t_{\mathrm{M}}}\right)+1\right]. \tag{23}$$

In the range of $0<\lambda<1$, the smaller the ratio of $\dfrac{t_{\mathrm{C}}}{t_{\mathrm{M}}}$, the more transverse deflection. If there are two pairs of piezoelectric elements for both sides of an elastic metal, the transverse deflection will be doubled. With the consideration of rigidity increase, the transverse deflections are given by,

$$\delta(x)=\frac{\varepsilon\varepsilon_0 S_{\mathrm{C}}V}{d_{31}E_eI_M}\cdot\frac{t_M+t_{\mathrm{C}}+2t_{\mathrm{S}}}{t_{\mathrm{C}}}l_{\mathrm{C}}\left(x-\frac{l_{\mathrm{C}}}{2}\right),\ E_e=E_{\mathrm{M}}+E_{\mathrm{S}}\frac{I_{\mathrm{S}}}{I_{\mathrm{M}}}+E_{\mathrm{C}}\frac{I_{\mathrm{C}}}{I_M},\ 0<x\le l_C \tag{24}$$

$$\delta(x)=\delta(l_C)+\frac{\varepsilon\varepsilon_0 S_{\mathrm{C}}V}{d_{31}EI_M}\cdot\frac{t_{\mathrm{M}}+t_{\mathrm{C}}+2t_{\mathrm{S}}}{t_{\mathrm{C}}}\cdot l_{\mathrm{C}}\left(x-\frac{l_C}{2}\right)$$

$$=\frac{\varepsilon\varepsilon_0 S_{\mathrm{C}}V}{d_{31}}\cdot\frac{t_{\mathrm{M}}+t_{\mathrm{C}}+2t_{\mathrm{S}}}{t_{\mathrm{C}}}\left[\frac{l_{\mathrm{C}}\left(l_{\mathrm{C}}-\frac{l_{\mathrm{C}}}{2}\right)}{E_{\mathrm{e}}I_M}+\frac{l_{\mathrm{C}}\left(x-\frac{l_{\mathrm{C}}}{2}\right)}{E\,I_{\mathrm{M}}}\right],\ E=E_M,\ l_C<x\le l \tag{25}$$

Therefore, the transverse deflection considering the rigidity increase at $x = l$ is given by.

$$\delta(l) = \frac{\varepsilon\varepsilon_0 S_C V}{d_{31}} \cdot \frac{t_M + t_C + 2t_S}{t_C} \left[\frac{l_C^2}{2E_e I_M} + \frac{l_C\left(l - \frac{l_C}{2}\right)}{E_M I_M} \right] \tag{26}$$

$\delta(l_c)$ in eq. (25) can be given from eq. (14).

$$\delta(l_c) = \frac{l_c^2}{2r} = l_c^2 \left(\frac{d_{31}\{D\}^T [AE]^{-1} \{E^p\}}{2 - \{D\}^T [AE]^{-1} \{T\}} \right) \tag{27}$$

where, $[AE] = \begin{bmatrix} \frac{1}{A_C E_C} & -\frac{1}{A_S E_S} & 0 & 0 & 0 \\ 0 & \frac{1}{A_S E_S} & -\frac{1}{A_M E_M} & 0 & 0 \\ 0 & 0 & \frac{1}{A_M E_M} & -\frac{1}{A_S E_S} & 0 \\ 0 & 0 & 0 & \frac{1}{A_S E_S} & -\frac{1}{A_C E_C} \\ 1 & 1 & 1 & 1 & 1 \end{bmatrix}$, $[T] = \begin{bmatrix} t_C + t_S \\ t_S + t_M \\ t_M + t_S \\ t_S + t_C \\ 0 \end{bmatrix}$,

$$[E^p] = \begin{bmatrix} -E^p \\ 0 \\ 0 \\ E^p \\ 0 \end{bmatrix} = \begin{bmatrix} -V/t_C \\ 0 \\ 0 \\ V/t_C \\ 0 \end{bmatrix}$$

For investigating the rigidity effects of bimorph piezoelectric actuator, the fundamental design parameters are shown in table 1. The material properties of components and the piezoelectric material properties are shown in table 2 and 3. The important characteristics due to the piezoelectric rigidity effects have influences on the angular displacement of mechanical dither. From the results, the feasible geometric dimensions of piezoelectric element can be studied and reflected in the fabrication of mechanical dithers. On the condition of $t_m^{\,L} \le t_m \le t_m^{\,U}$, the angular displacements of the mechanical dithers are calculated. Under the electrical signals, the angular velocities are investigated through the relative angular displacement sensor. Each mechanical dither is designed for being operated at intervals of 20 Hz. Using the numerical equations, the angular displacement of mechanical dithers are compared in table 4. In table 4, the calculated resonant frequencies from numerical equation are within the relative errors of 1 %.

Table 1. Fundamental design parameters of bimorph actuator

Design parameter	Value (mm)
Center of piezoelectric element (a_1)	$l_C/2 + 1.5$
Length of metal pressure-sensitive element ($l_M = l$)	21
Thickness of metal pressure-sensitive element (t_M)	2.94, 3.08, 3.22
Width of metal pressure-sensitive element (w_M , w_C)	5
Thickness of piezoelectric element (t_C)	0.3 ~ 0.7
Length of piezoelectric element (l_C)	$0.25\,l_M$ ~$0.9\,l_M$

Table 2. Mechanical material properties of components

Materials	Elastic modulus (GPa)	Poisson's ratio	Density (kg/m^3)
Metal	144.9	0.29	8110
Piezoelectric element	40	0.30	7700
Connective seam	15	0.31	1800

Table 3. Piezoelectric material properties of piezoelectric layer

Material properties	PZT
Piezoelectric constants (10^{-12} m/V)	
d33	-250
d31	2500
d32	0
Relative permittivity *e/e0*	
(e0=8.854x10^{-12} F/m)	5500

Table 4. Deflection of mechanical dither spokes of various thicknesses

Type	Thickness t_M (mm)	Test deflection (mm)	Deflection (mm) using eq. (24)	Deflection. (mm) using eq.(27)
1	2.94	2.595	2.591	2.596
2	3.08	2.449	2.443	2.454
3	3.22	2.300	2.291	2.304

Conclusion

This paper presents the general modeling method of multilayer structure with *m*-layers. A model describing the deflection of a piezoelectric multi-morph structure can be derived by using the basic mechanics principles of static equilibrium and strain compatibility between the interfacial layers. Using this formulation, the layer selection and distribution is easy in designing the layered model. The change from one configuration to another can be represented by a change of the related modification of the assignments of equivalent material parameters to the different sub-layers. And, the geometric dimensions such as thickness, width and height in the materials can be studied for the improvement of static or dynamic stiffness. In the numerical equations, the nominal material properties of piezoelectric elements and seam elements are generally used, but they have the probabilistic distributions of material properties. In the consideration of the probabilistic distributions of material properties, the presented equations are available for the structural characteristics.

REFERENCES

Agnes, G. S., Single-element modeling of multiplayer constrained-layer damping treatments, *Proceedings of SPIE-The International Society for Optical Engineering*, 1995, 2445

DeVoe D. L. and Pisano A. P.; Modeling and optimal design of piezoelectric cantilever microactuators, *Journal of Microelectromechanical systems,* 1997, 6(3), 266-270

Hwang W. S. and Park H. C. Finite element modeling of piezoelectric sensors and actuators, *AIAA Journal, 1993,* 31(5), 930-937

Lee, D. C. A design of panel structure for the improvement of dynamic stiffness, *Proc. Instn. Mech. Engrs. Part D; Journal of Automobile engineering*, 2004, 218(6), 647-654

Lee, D. C. Yun, D. W. Han, C. S. A material rigidity effect of a bimorph piezoelectric actuator, *Smart Materials and Structures,* 2007, *16(4),* 1043-1049

Lee, D. C., Choi, H. S., Han, C. S., Jeong, H. J. A compensation of Young's modulus in polysilicon structure with discontinuous material distribution, *Material Letters,* 2005, *59(29)*, 3900-3903

Lee, D. C., Jang, J. H., Han, C. S. Parametric design consideration of a vibro-elastic bimorph piezoelectric converter for a ring laser gyroscope, *Smart Materials and Structures,* 2006, *15(5)*, 1165-1171

Nashif, A.; Jones, D.; Henderson, J.; *Vibration damping*, 2nd Ed.; John Wiley & Sons, Inc.: New York, USA, 1985

Oka, Y., Ono H. and Hirako N.; Panel vibration control for booming noise reduction, *Proceedings of Noise and Vibration Conferences, SAE P-244*, 1991, 427-433

Ross, D., Unger, E. E., Kerwin, E. M. Jr.; Damping of plate flexural vibrations by means of viscoelastic laminate, *Structural Damping, ASME*, 1959, 49-99

Uchino K. Piezoelectric Actuators and ultrasonic motors, Kluwer Academic Publishers; Massachusetts, USA, 1997

Ugural, A. C., Fenster, S. K. *Advanced strength and applied elasticity*, 3rd Ed.; Prentice-Hall: New Jersey, USA, 1995

Vetrov, A. A., Volkonskii, V. B., Svistunov, D. V. Calculation, fabrication, and study of waveguides for an integrated-optics gyroscope *Journal of optical technology*, 1999, *66(5)*, 428-433

Wang Q. M. and Cross L. E.; Contitutive equations of symmetrical triple layer piezoelectric benders, *IEE Transactions of Ultrasonics, Ferroelectronics and Frequency Control*, 1999, 46(6) 1343-1351.

****